17

On-line corrosion monitoring of indoor atmospheres

L. SJÖGREN, Corrosion and Metals Research Institute, Stockholm, Sweden and
N. LE BOZEC, Institut de la Corrosion, Brest, France

17.1 Introduction

Investigations have shown that risks of indoor corrosion are more easily and more reliably estimated by exposing metals, as compared with analysing climatic conditions and air pollutant concentrations [1]. Such methods are employed for environmental classification, as described by international [2] and business [3, 4] standards. Methods stated in the standards referred to are not for continuous monitoring. Electrical Resistance (ER) sensors and the quartz crystal microbalance (QCM) are commercially available methods used for on-line measurements in process industry control rooms and in museums. The use of resistance sensors in control and storage rooms has been described by Johansson and Leygraf [5]. Use of the quartz crystal microbalance for monitoring corrosivity under mild atmospheric conditions has been described by Zakipour and Leygraf [6] and its use for environmental characterisation of control rooms by Forslund *et al*. [7].

The aim of this investigation was to evaluate the performance of commercially available corrosion monitoring instruments and sensors. A second aim was the development of a small battery-operated corrosion logger suitable for permanent or temporary use at various indoor locations.

17.2 Experimental

17.2.1 Quartz crystal microbalance (QCM)

A quartz crystal microbalance measures corrosion as changes in resonance frequency of a piezo-electric quartz crystal with a metal coating, the resonance frequency being a function of the mass of the crystal; see Fig. 17.1. Most crystals used for this application are of the so-called AT-cut, the disc being cut at an angle of +35°15′ relative to the crystallographic *Z*-axis of the original single crystal. This results in a shear deformation of the crystal with a stable and sharp resonance frequency. The temperature dependence of the

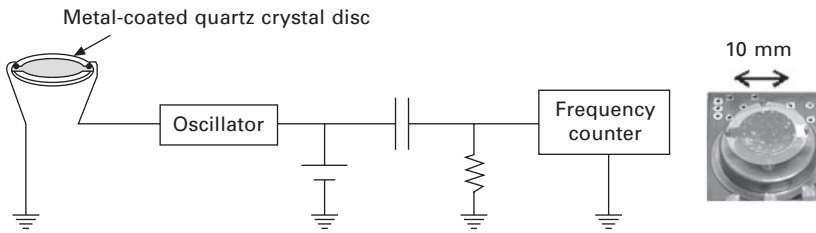

17.1 Principle of the quartz crystal microbalance and photo of a copper-coated crystal disc after exposure.

resonance frequency is slight at about 25°C, which is convenient for indoor applications. Crystals for corrosion measurements are coated by the metal of interest, usually by physical vapour deposition.

The frequency response from changes in mass follows the Sauerbrey equation (17.1):

$$\Delta f = -\left(\frac{f_0^2}{\rho_q N}\right)\Delta m \qquad 17.1$$

where: Δf = change in frequency
f_0 = resonance frequency
ρ_q = density (2.648 g/cm^3 for quartz)
N = frequency constant (1670 kHz mm for a transverse wave in AT-cut quartz)
Δm = mass change/area, assuming film growth on one side of the crystal.

A frequency change of 1 Hz for a 5 MHz crystal (readily measurable) corresponds to 18 ng/cm^2, giving a film thickness resolution of 2 Å for a Cu_2S film [6, 8]. A disadvantage of the quartz crystal method is that it is equally sensitive to dust and other contaminants as to corrosion products formed. Further, water is adsorbed on the surface, adding to the mass of the crystal and to sensor response. The amount of water depends on relative humidity, metal coating, surface roughness and surface films present [9, 10].

Commercial instruments with 6 MHz quartz crystal sensors, coated with 4000–5000 Å copper or silver, were used in this investigation. The instruments measure resonance frequency, and the results obtained are reported as film growth, assuming corrosion films of copper and silver sulphide (Cu_2S and Ag_2S) respectively.

17.2.2 Electrical resistance sensors

With this method, resistance of a thin track of metal was measured. Corrosion, reducing the metal thickness, causes resistance to increase. The method

requires the sensing metal to corrode uniformly; metals prone to pitting, crevice or grain boundary corrosion, under the conditions to be monitored, are not usable. The sensors employed in this investigation consisted of serpentine copper or silver tracks, deposited on a glass substrate; see Fig. 17.2. By measuring relative to a corrosion-protected track of the same metal and at the same temperature, the temperature dependence of the metal resistivity was compensated for. The corrosion rate is calculated according to equation 17.2:

$$\text{Corrosion depth} = t_i\left(1 - \frac{R_{ref}}{R_s} \cdot \frac{R_{i,s}}{R_{i,ref}}\right) \qquad 17.2$$

where: t_i = initial metal track thickness (assumed equal for the reference and sensor tracks)
R_s = resistance of the sensor track
R_{ref} = resistance of the reference track
$R_{i,s}$, $R_{i,ref}$ = initial resistance of sensor- and reference track respectively.

Besides the accuracy of the resistance meter, sensitivity is governed by metal track length, width and thickness. It is thus possible to produce sensors with a sensitivity and life adapted to the specific requirements.

Measurements were performed using a logging instrument storing results for up to four resistance sensors, connected via cables. Additional measurements were performed manually, using a resistance bridge or a microohmmeter. In both cases, measurement current was less than 1 mA and current pulses were

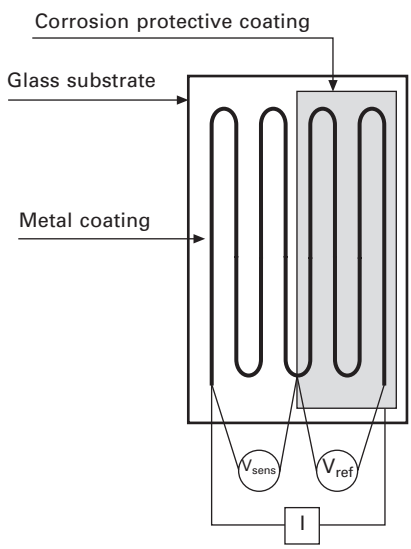

17.2 Principle of the electrical resistance sensor.

used for thermo potential compensation. Properties of commercially available resistance sensors with 2 mm wide and 5000–6000 Å copper or silver tracks, and of laboratory-manufactured sensors (Acreo, Norrköping, Sweden) with 1 mm wide, 4300 Å thick sputtered copper tracks or 3900 Å thick evaporated silver tracks, were evaluated.

17.2.3 Prototype corrosion logger

A small battery-operated corrosion logger was developed for enabling measurements to be made in confined spaces or where electricity is unavailable, e.g. in display cases, in cabinets intended for storage of sensitive objects or inside transport packages. The logger, shown in Fig. 17.3, employs the electrical resistance technique. It has been evaluated with laboratory-manufactured sensors with copper and silver tracks.

17.2.4 Reference methods

For field exposures and some laboratory exposures, reference coupons of silver and copper were employed. The coupons were degreased and ground with 1200 P (600 grit) SiC paper. The coupons were weighed relative to a reference weight before and after exposure; approximate weighing accuracy is $\pm 0{,}15\ \mu g/cm^2$. In some cases, besides mass gain, mass loss was determined for copper coupons after removal of the corrosion products in 5 wt% sulphamic acid, H_2NSO_3H. For silver, coulometric reduction was employed, following the method described by Krumbein *et al*. [11].

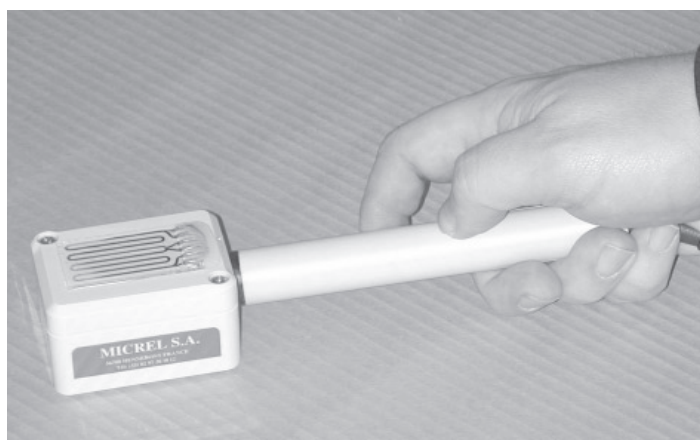

17.3 Taking readings from a prototype corrosion logger.

17.2.5 Laboratory exposures

Sensors and metal coupons were exposed in a climatic cabinet under varying temperature and humidity conditions, with and without corrosive gases. Sulphur dioxide, hydrogen sulphide and/or nitrogen dioxide in low concentrations, e.g. from a few ppb to 100 ppb, were used as corrosive gases.

17.2.6 Field exposures

Three different exposure sites were employed, all at pulp and paper plants. At the first site, sensors were mounted inside ventilation shafts, one before and one after a carbon filter cassette for incoming air. At the second site, sensors were positioned on top of a cabinet, directly exposed to incoming purified air, inside a room for a distribution plant of a cardboard mill. The third site was inside a pump room in a building located beside a sewage plant, the sensors being positioned approximately 1 m above the floor.

17.3 Results and discussion

For exposures including both quartz crystals and resistance sensors, measurement results for the different sensors and metal coupons were transformed to film growth, as measured from the start of each exposure. The film thickness is calculated according to equation 17.3:

$$\text{Thickness of corrosion film} = \text{Corrosion depth} \times \frac{\rho(\text{metal})}{\rho(\text{film})} \times \frac{1}{n(\text{metal/film})} \times \frac{\text{Mw(film)}}{\text{Mw(metal)}} \qquad 17.3$$

where: ρ = density (of corrosion film or metal)
n (metal/film) = metal equivalents per film equivalent (e.g. 2 for Cu_2S)
Mw = molecular weight.

For calculating film thickness, films on copper are assumed to consist of copper sulphide Cu_2S and films on silver of silver sulphide Ag_2S, in accordance with the presentation of the quartz crystal sensor results – see paragraph 17.2.1. Since corrosion products formed under benign conditions are normally not sulphides, this assumption will result in incorrect film growth results. As an example, if the dominant constituent of the corrosion film is $Cu_4SO_4{*}(OH)_6$, measuring corrosion as mass loss or via changes in electrical resistance and assuming that the film is Cu_2S will result in a calculated film thickness of half its true value – see Table 17.1.

Table 17.1 Film thickness calculations from corrosion depth

Copper corrosion product	Film thickness (Å) for a corrosion depth of 1Å	Silver corrosion product	Film thickness (Å) for a corrosion depth of 1Å
Cu_2S	2.0	Ag_2S	1.7
CuS	2.9	AgCl	2.5
Cu_2O	1.7	Ag_2O	1.6
CuO	1.7	Ag_2SO_4	2.8
$Cu_4SO_4*(OH)_6$	4.0		

Note: Under indoor conditions mixtures of different carboxylate salts are reported to be formed on copper surfaces, i.e. even larger molecules than used in the examples of the table. On silver, Ag_2S is common [12].

Table 17.2 Corrosion depth calculations from mass gain

Copper corrosion product	Corrosion depth (Å) for 1 mg/m^2 mass gain	Silver corrosion product	Corrosion depth (Å) for 1 mg/m^2 mass gain
Cu_2S	4.4	Ag_2S	6.4
CuS	2.2	AgCl	2.9
Cu_2O	8.9	Ag_2O	12.8
CuO	4.5	Ag_2SO_4	2.1
$Cu_4SO_4*(OH)_6$	1.4		

Measuring mass gain, corrosion depth can be calculated according to equation 17.4:

$$\text{Corrosion depth} = \text{Mass gain} \times \frac{1}{\rho(\text{metal})} \times \frac{\text{Mw(metal)} \times n(\text{metal/film})}{\text{Mw(film)} - \text{Mw(metal)} \times n(\text{metal/film})} \quad 17.4$$

Examples are given in Table 17.2. If mass gain from growth of a $Cu_4SO_4*(OH)_6$ film is measured using the QCM and is presented as film thickness assuming Cu_2S, this would correspond to overestimating the corrosion depth by a factor of 3.

17.3.1 Laboratory exposures, commercial instruments and sensors

As expected, readings from the quartz crystal sensors are affected by both humidity and temperature, with individual differences in magnitude:

Fig. 17.4 (a). Readings from electrical resistance sensors have shown no humidity dependency but effects of temperature, despite the use of a reference for temperature compensation. As shown in Fig. 17.4 (b), the temperature effects differ between individual sensors and between metals used, silver showing the most pronounced effects.

Examples of results from laboratory exposures in humid air, with corrosive gases added, are presented in Fig. 17.5. Differences in slopes of the individual graphs reflect the spread in sensor response. The ability to indicate changes in test conditions is shown as changes in the slope of the graphs. Even if individual differences are large, all sensors reveal changes in exposure conditions. Differences in behaviour of the two metals are evident, copper showing higher sensitivity to humidity and temperature changes while silver is more affected by the addition of corrosive gases. For copper, corrosion rate increases when humidity increases, while silver corrosion is indicated

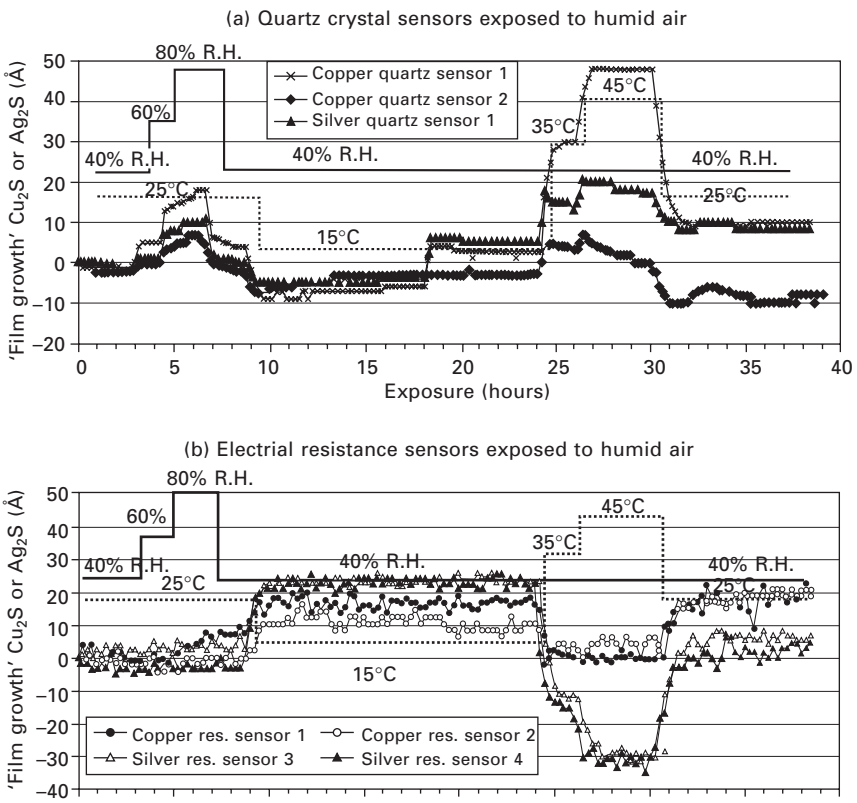

17.4 (a) Quartz crystal, and (b) commercial electrical resistance sensors, temperature and humidity effects. Readings are expressed as film growth – corresponding Cu_2S or Ag_2S film thickness as if the readings were due to corrosion.

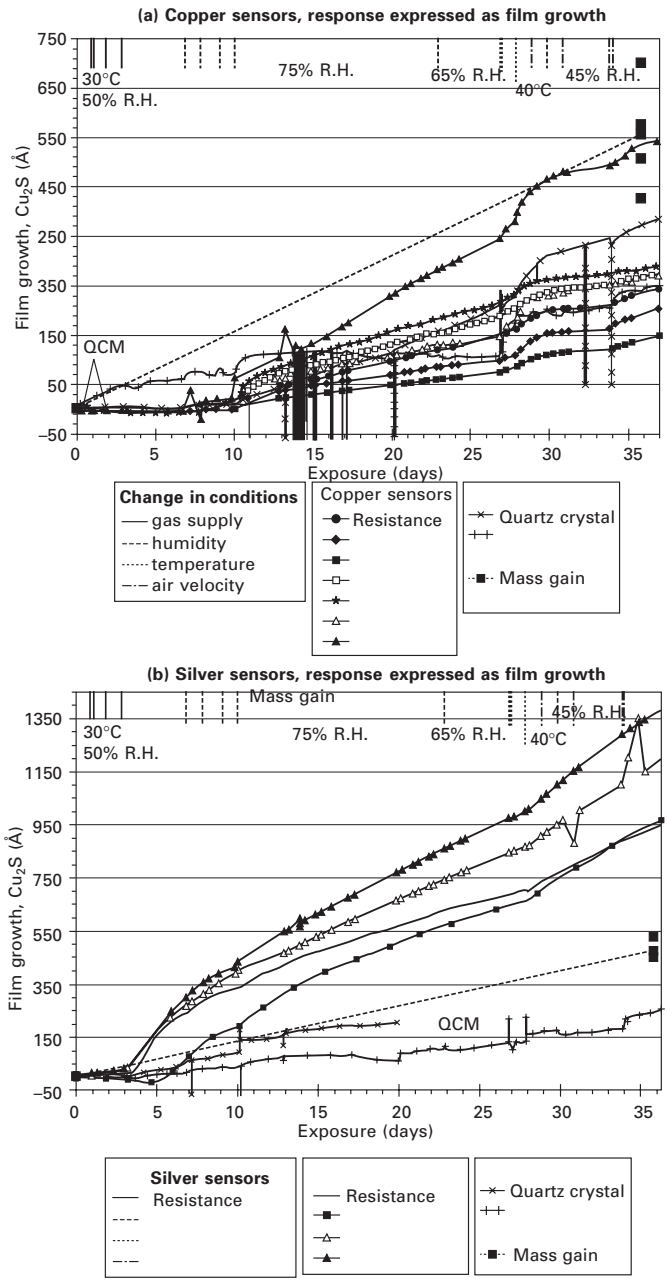

17.5 Exposure of (a) copper and (b) silver sensors in humid air, 65–75% R.H., 30–40°C with low concentrations of NO_2, SO_2 and H_2S (approx. 50 ppb SO_2 and NO_2, 2–3 ppb H_2S, gases added one by one during the first three days). Curve symbols mark manual measurements while curves without symbols show results from logging data every 15 minutes.

also at lower humidity. Measurement disturbances do occur for both types of sensors, as also shown in Fig. 17.5.

17.3.2 Field exposures, commercial instruments and sensors

In dusty environments, such as before the carbon filter in a ventilation shaft, Fig. 17.6, effects of dust are far greater than effects of corrosion. Quartz crystal sensors are thus not very useful under such circumstances. The resistance sensors show that corrosivity is indeed lower after the carbon filter. It is evident from mass gain and quartz crystal results that the amount of dust is much lower after the filter, through it still seems too high for the quartz sensor to give useful results. Based on electrical resistance sensor and mass loss results, corrosivity is estimated as low (G1 according to ISA–S71.04-1985 [3], a corrosivity classification system for electronic equipment) both before and after the carbon filter.

Results from sensors exposed in a distribution plant and in a pump room, at both a pulp and a paper plant, are shown in Fig. 17.7. The relation between the different types of sensors is similar to the laboratory exposure with low concentrations of corrosive gases, Fig. 17.5. Compared to resistance sensors, relatively higher copper corrosion rates are indicated by mass gain. A reason may be that corrosion products with larger, thus heavier, molecules than Cu_2S, the substance assumed for the film thickness calculations, are formed

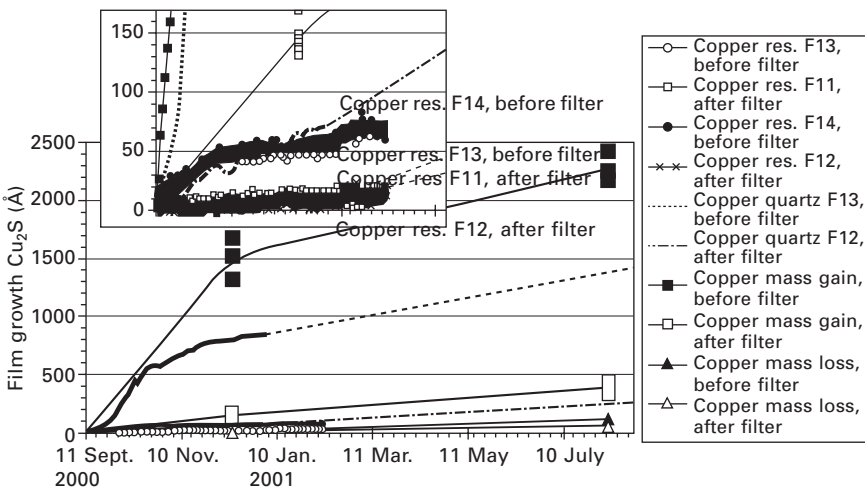

17.6 Exposure of copper sensors in ventilation shafts before and after a carbon filter. Mass gain curve symbols indicate the metal coupon being exchanged. The resistance sensors were removed after half the exposure period.

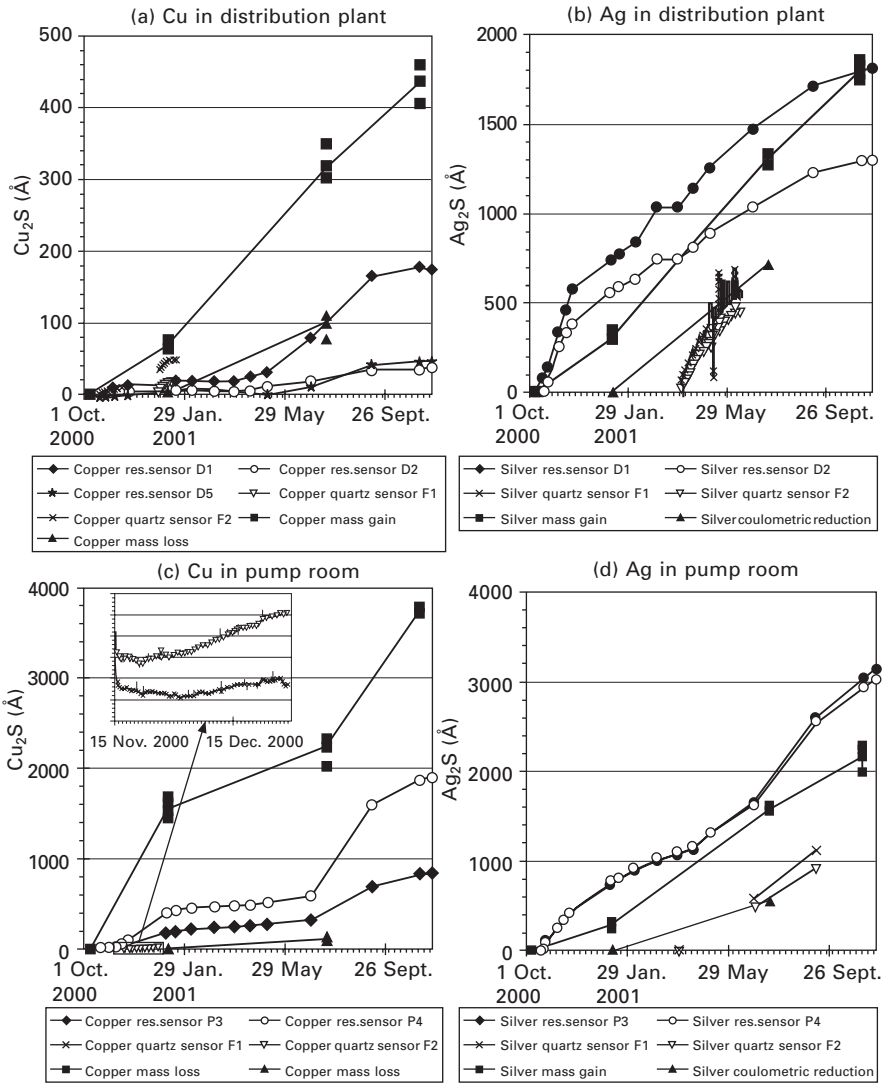

17.7 Exposure of copper and silver sensors in the distribution plant and pump room. Measurement results are expressed as film growth. Mass gain curve symbols indicate the metal coupon being exchanged. The quartz crystal sensors were alternately exposed in the two rooms.

in the low gas concentration test and in the field (Cu_2S is expected to form under more corrosive conditions).

In the exposures of Fig. 17.7, the quartz crystal sensors and instrument were moved between the two locations, a procedure that seems to affect readings. Moving the copper quartz sensors from the distribution plant to the pump room resulted in a diversion between the two individual sensors. When

moved back to the distribution plant, the two sensors follow the same path, but are now parallel. The copper quartz sensors were later exchanged for silver ones. Due to an instrumental problem, however, it was only possible to obtain information on average film growth rate for silver sensors in the pump room; these results, for silver quartz sensors F1 and F2, are presented as broken lines in Fig. 17.7 (d). Employing the broken line as quartz crystal results, the three methods for measuring silver corrosion (compare the slopes of the curves) show much better agreement when compared to the copper sensor results.

From Fig. 17.7 it is obvious that corrosivity is higher in the pump room than in the distribution plant, copper showing the largest difference. A higher corrosion rate is further indicated during the summer period in the pump room; this may be due to higher summer temperatures or to variations in wind direction, the windows of the room facing a sewage plant. The increase in corrosivity in the distribution plant registered by the resistance sensors in the spring may be due to activities preparing for a planned shutdown, activities involving open doors, and the making of a hole in the floor.

Based on copper sensor and mass gain results, corrosivity is estimated as low in the distribution plant, e.g. G1 according to ISA–S71.04-1985 [3]. Silver corrosivity is higher, entailing risks for deteriorated silver-plated connectors, for example. In the pump room, copper corrosivity is low to moderate, e.g. G1–G2 corrosivity category, which can be regarded as a borderline case for electronic equipment. Silver corrosivity is equivalent to that measured in the distribution plant.

17.3.3 Laboratory exposure, prototype logger, laboratory manufactured sensors

Results from a laboratory exposure to cyclic humidity, including low concentrations of NO_2, are shown in Fig. 17.8, illustrating differences between the two metals in reacting to changes in environmental conditions. Copper sensors appear more sensitive to changes in NO_2 concentration while silver sensors show stronger reactions to temperature variations. With the prototype corrosion logger and the approximately 4000 Å copper and silver sensors, measurement sensitivity is estimated at a few angstroms reduction in thickness, which should be sufficient for corrosion rate measurements under benign indoor atmospheric conditions.

Figure 17.9 shows results from several copper and silver sensors exposed in parallel, including both logger readings and manual readings. For the manual silver sensor readings, average corrosion rate was calculated for two exposure periods and is presented in the diagram. A standard deviation of 26% and 13% was obtained for the two exposure periods respectively. This variation in sensor response is considered acceptable for corrosivity

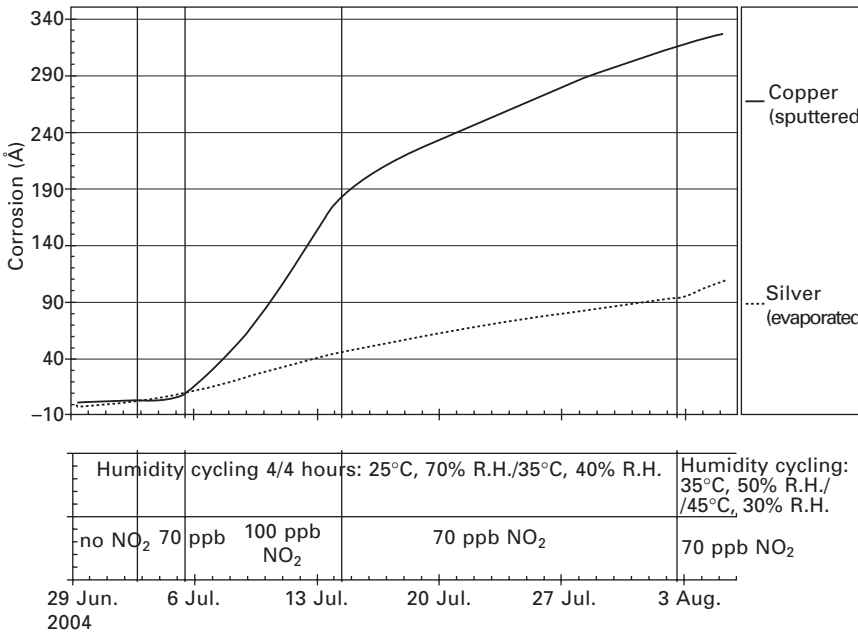

17.8 Corrosion logger results presented as corrosion depth, for copper and silver sensors exposed to humidity and temperature cycling and low concentrations of NO_2. If films of Cu_2S and Ag_2S are assumed to be formed, the corrosion film thickness (in Å) would be approximately twice the corrosion depth (see Table 17.1).

classification purposes, even if variations in response from mass gain measurements are generally smaller – compare Fig. 17.7.

Since a couple of copper sensors showed substantially deviant behaviour, no statistical evaluation of the copper sensors has been performed. The deviant behaviour, characterised by sudden large increases in measured corrosion rate, is explained by local attack. Protruding corrosion products are clearly visible at 10× magnification; the attack resulted in a substantial reduction in metal thickness across a small part of the copper track. The attack is believed to have been initiated by dust particles which, being hygroscopic, would be more corrosive to copper than to silver, thus explaining why this effect was observed only for copper.

As shown in Fig. 17.9, the logger readings were lower than the manual readings, for both metals. A likely explanation for this behaviour is differences in voltage instrument response between the sensor and reference tracks, a problem not relevant for the manual measurements where the same instrument circuitry was used for both tracks. This problem should be easily corrected in future developments of the logger.

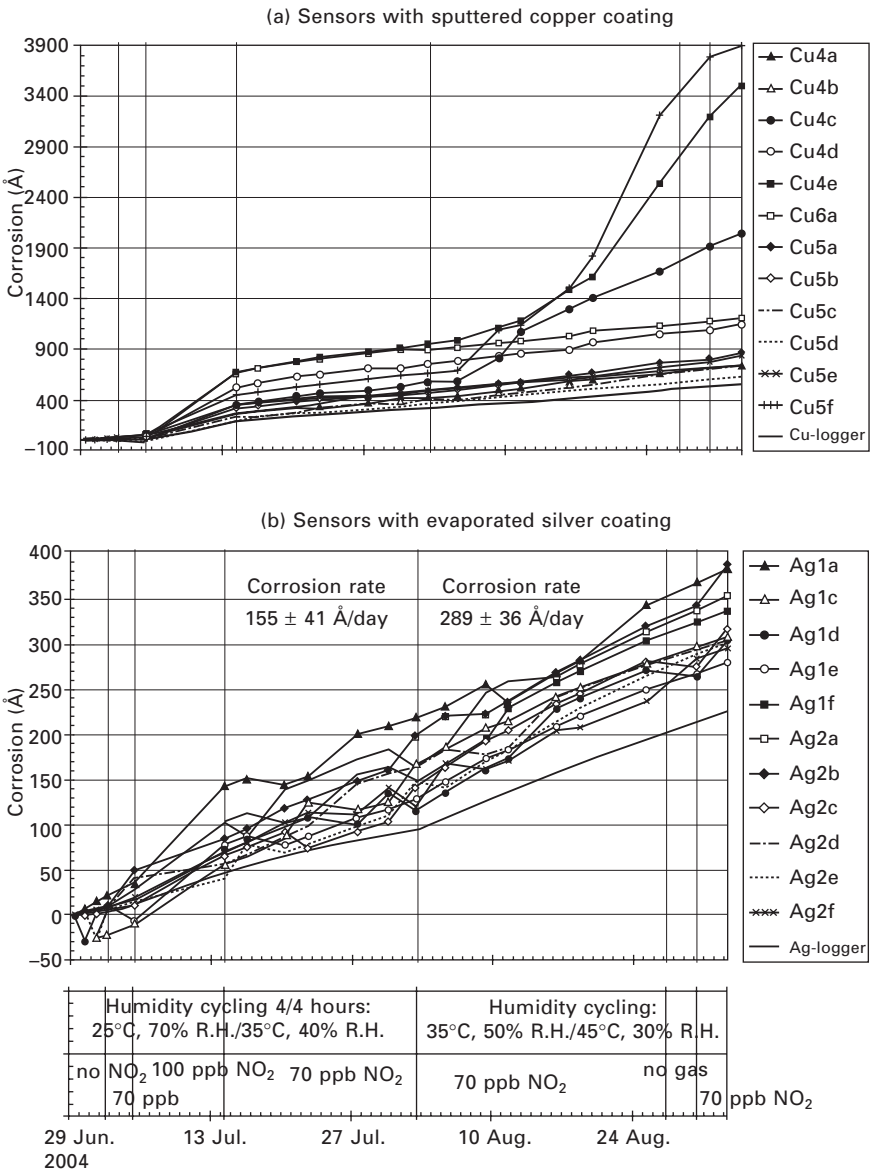

17.9 (a) Copper and (b) silver sensor results presented as corrosion depth. The sensors were exposed to humidity and temperature cycling in presence of low concentrations of NO_2. If films of Cu_2S and Ag_2S are assumed to be formed, the corrosion film thickness (in Å) would be approximately twice the corrosion depth (see Table 17.1).

17.4 Conclusions

The monitoring methods evaluated, quartz crystal microbalance and electrical resistance sensors, are both found to be useful for monitoring changes in environmental conditions and to be sufficiently sensitive for use under indoor atmospheric conditions. Both sensor types can be used for measuring corrosion rates of different metals, provided corrosion is uniform.

Electrical resistance sensors measure corrosion, i.e. metal loss, directly and can be adapted for use under various corrosivity conditions. These sensors are not directly affected by particles, water films, etc., and are thus considered most suited for general use. With approximately 4000 Å thick copper or silver tracks, it has been possible to achieve a measurement sensitivity of 1–2 Å corrosion (reduction in thickness). The reproducibility of sensor response is considered acceptable for the silver sensors with <30% standard deviation for corrosion rate measurements during laboratory exposures. The copper sensors require further development, optimising track dimension, in order to reduce effects of local attack, e.g. caused by dust particles.

The small battery-operated corrosion logger that has been developed, working with resistance sensors, offers sufficiently high measurement sensitivity for detecting changes and differences in corrosion rate under indoor conditions, with the advantage of giving on-line information. The logger is thus suited for comparing conditions at different locations and is small enough for monitoring corrosive conditions, e.g. inside packages during transport.

17.5 Acknowledgement

The authors wish to express their thanks to Conseil Régional de Bretagne for supporting the development of the prototype corrosion logger.

17.6 References

1. E. Johansson, B. Rendahl, V. Kucera, *Corrosion 98*, San Diego, paper 359.
2. ISO 9223, 'Corrosion of metals and alloys – Corrosivity of atmospheres – Classification', International Organization for Standardization, Geneva (1992).
3. ISA-S71.04-1985, 'Standard. Environmental conditions for process measurements and control systems: Airborne contaminants', Instrument Society of America, Research Triangle Park, NC (1985).
4. SSG 4251E, 'Electrical operations rooms. Air treatment plants. Project engineering instructions', Pulp and Paper Industries' Engineering Co. (1994).
5. E. Johansson, C. Leygraf, *British Corrosion Journal*, vol. 34, no. 1 (1999), p. 27.
6. S. Zakipour, C. Leygraf, *British Corrosion Journal*, vol. 27, no. 4 (1992) p. 295.
7. M. Forslund, J. Majoros, C. Leygraf, *Journal of the Electrochemical Society*, vol. 144, no. 8 (1997) p. 2637.
8 T. Aastrup, C. Leygraf, *Journal of the Electrochemical Society*, vol. 44, no. 9 (1997) p. 2986.

9. M. Forslund, C. Leygraf, *Journal of the Electrochemical Society*, vol. 44, no. 1 (1997) p. 113.
10. T. Aastrup, '*In situ* investigations of the metal/atmosphere interface', Doctoral Thesis, Department of Materials Science and Engineering, Division of Corrosion Science, Royal Institute of Technology, S-100 44 Stockholm, Sweden (1999).
11. S.J. Krumbein, B. Newell, V. Pascucci, *Journal of Testing and Evaluation*, vol. 17 (1989), p. 357.
12. D. Persson, C. Leygraf, *Journal of the Electrochemical Society*, vol. 142, no. 5 (1995), p. 1468.